TEMPORAL ACCELERATION IN HYPERPOLARIZATION IMAGING USING IMAGE-DOMAIN COMPRESSED SENSING

B. SHARIF[1], D. LI[1,2], AND S. WAGNER[1]
[1]BIOMEDICAL IMAGING RESEARCH INSTITUTE, CEDARS-SINAI MEDICAL CENTER, LOS ANGELES, CA, UNITED STATES,
[2]NORTHWESTERN UNIVERSITY, CHICAGO, IL, UNITED STATES

INTRODUCTION

Since the introduction of the Fourier transform (FT) into MR spectroscopy the read time has been considered to have no associated cost due to the longitudinal-relaxation wait time. In a conventional imaging sequence a delay time is typically present to establish a steady state magnetization. Hyperpolarization has introduced a new paradigm [1]. In hyperpolarization imaging the magnetization can be 10,000 times the normal thermal equilibrium magnetization. However, loss of magnetization is continuous owing to T1 relaxation. Variable angle (VA) pulses are employed to maintain a constant signal return [1,2]. With VA acquisition methods, the fixed signal return for each phase-encode (PE) sampling will be greater if the total acquisition time is reduced [3]. Additionally, if the total acquisition time exceeds the T1 of the hyperpolarized molecule observed, reducing the number of PEs will increase the signal. Recently, the potential of compressed sensing (CS) [4,5] with pseudo-random sampling [6] has been demonstrated for MR spectroscopic imaging [2] — and also for lung imaging [7]. In this work, we demonstrate that a two-fold (R=2) gain in sampling can be achieved — with little compromise on image quality — by exploiting the image-domain sparsity in two-dimensional ^{13}C hyperpolarization imaging. The utilized CS scheme exploits the sparsity in the image domain rather than some transform domain [6]. To achieve this objective, we employ a modified pseudo-random Cartesian sampling scheme with undersampling in both PE and frequency-encode (FE) directions.

METHODS

For 2D Cartesian CS imaging, the k-space acquisition scheme is typically taken to be similar to the sampling pattern S1 shown in the adjoining figure (33x32 k-space matrix). Specifically, a subset of the PE lines (within the Nyquist grid) are selected in a pseudo-random fashion (typically, with higher sampling density in the central k-space). The figure also shows an alternative pseudo-random sampling scheme S2, which differs with S1 in that both PE and FE dimensions of the k-space are subsampled. Implementation of an acquisition pulse sequence according to S2 is somewhat more complicated that S1. Specifically, compared to S1, in S2 a slice rotation (a PE/FE gradient switching) will also be needed — which is feasible, e.g., in GRE.

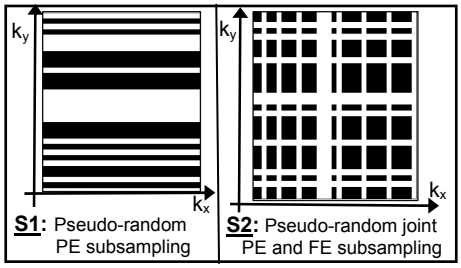

Ten datasets of ^{13}C imaging of hyperpolarized succinate were used for evaluation of image-domain CS with 12 different S1-type subsampling patterns (including the depicted one) in addition to the S2 pattern shown here. Data was obtained with a Bruker 4.7T scanner using a low flip angle with a surface coil encompassing a 1 cm tumor (renal or lymphoma) implanted on the back of the mice. A gradient-echo sequence with an echo time of 7.9 ms and a repetition time of 96 ms was used to obtain a single 1 cm slice (FOV: 6x6 cm) with a 33 x 32 image matrix. To simulate CS undersampled acquisition data subsampling was used. To perform the CS reconstruction, we apply an iterative reweighed least squares algorithm to implement the basis pursuit (BP) technique [5]. The BP reconstruction algorithm optimizes the following functional: $\hat{g} = \arg\min_g\{\|d - Fg\|_2^2 + \alpha\|g\|_1\}$, where g is the unknown image in the (x,y) domain, d is the collected data, F denotes the subsampled 2D discrete FT operator (e.g., S1 or S2), and α is the Lagrangian multiplier in the BP problem setup, which controls the trade-off between data fidelity and image-domain sparsity of $\hat{g}$. For comparison, a pseudo-inverse "linear" reconstruction was also computed.

RESULTS

Two sets of reconstruction results with 2-fold subsampling are shown on the right (one row for each tumor type). The reconstructed 33x32 images were interpolated using cubic splines to match the conventional visualization scheme (same gray scale). The overlaid box on the full FOV original image (no subsampling) shows the location of the zoomed-in images. The 3rd column shows the CS (BP) result corresponding to the best of the 12 generated S1-type subsampling patterns. The 4th and 5th columns correspond to the S2 subsampling scheme (linear and BP). The mean squared error (MSE), defined relative to the fully encoded image, was computed for each full-FOV image and also for "region-of-interest" (ROI), defined to be those pixels that have an intensity of at least 10% of the peak value. The set of MSE values for all 10 datasets are plotted below for BP reconstruction corresponding to S1 and S2.

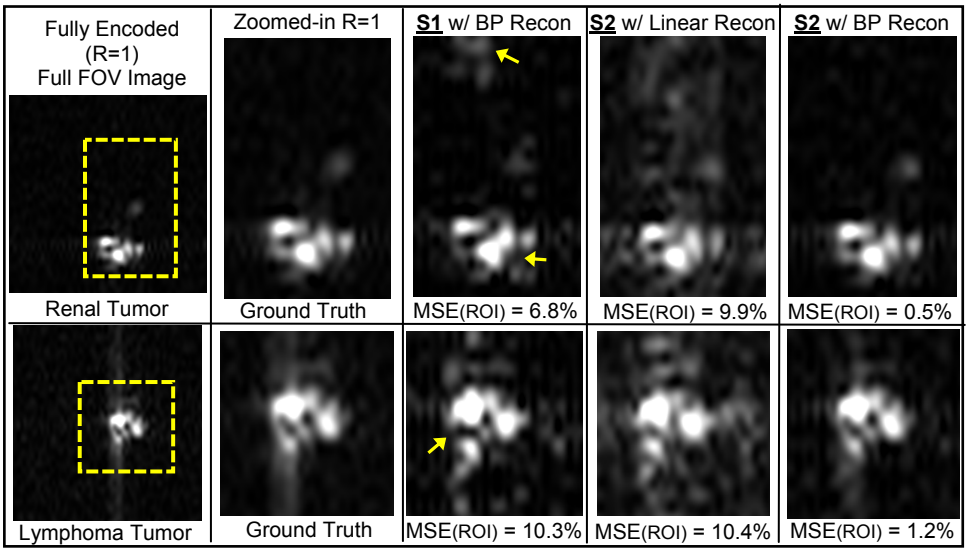

DISCUSSION

As can be seen from the reconstruction results, S1-type subsampling leads to significant artifacts (highlighted by arrows) and linear reconstruction performs poorly. In contrast, S2 subsampling (with BP reconstruction) achieves very good image quality. Considering the MSE plots in the adjoining figure, it is seen that S2-type subsampling consistently outperforms S1 and overall achieves very good MSE, especially in the ROI (MSE<2.1% in ROI). Based on the PSF analysis framework for CS [6], the improved performance for S2 can be attributed to the fact that with S1, subsampling is restricted to 1D (only PE) whereas S2 performs subsampling in 2D; hence, it spreads the PSF in 2 rather than 1 dimensions (however, S2 is more limited than 3D acquisition). The temporal acceleration gained through undersampling (R=2) will enable higher resolution full-body imaging of hyperpolarized biomarkers for cancer detection and monitoring — a key technique for translational medicine.

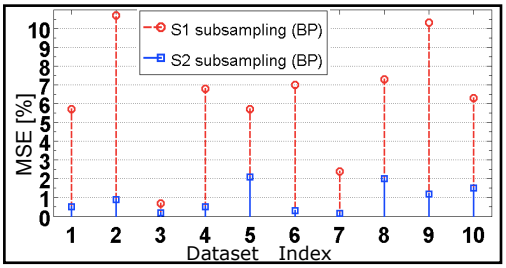

REFERENCES [**1**] Zhao et al. JMR B 1996; 113:179-83. [**2**] Hu et al. JMR 2008; 192:258-64. [**3**] Wagner et al., ISMRM 2009, p. 2668. [**4**] Donoho, IEEE Trans. IT 2006; 52:1289– 1306. [**5**] Donoho et al., IEEE Trans. IT 2006; 52:6-18. [**6**] Lustig et al., MRM 2007; 58:1182-95. [**7**] Ajraoui et al., MRM 2010; 63:1059-69.